



Published as: *Nature*. 2010 February 11; 463(7282): 808–812.

Role of conserved non-coding DNA elements in the *Foxp3* gene in regulatory T-cell fate

Ye Zheng^{1,2,*†}, Steven Josefowicz^{1,2,*}, Ashutosh Chaudhry^{1,2}, Xiao P. Peng², Katherine Forbush¹, and Alexander Y. Rudensky^{1,2}

¹Howard Hughes Medical Institute and Department of Immunology, University of Washington, Seattle, Washington 98195, USA

²Howard Hughes Medical Institute and Immunology Program, Memorial Sloan-Kettering Cancer Center, New York, New York 10065, USA

Abstract

Immune homeostasis is dependent on tight control over the size of a population of regulatory T (T_{reg}) cells capable of suppressing over-exuberant immune responses. The T_{reg} cell subset is comprised of cells that commit to the T_{reg} lineage by upregulating the transcription factor *Foxp3* either in the thymus (tT_{reg}) or in the periphery (iT_{reg})^{1,2}. Considering a central role for *Foxp3* in T_{reg} cell differentiation and function^{3,4}, we proposed that conserved non-coding DNA sequence (CNS) elements at the *Foxp3* locus encode information defining the size, composition and stability of the T_{reg} cell population. Here we describe the function of three *Foxp3* CNS elements (CNS1–3) in T_{reg} cell fate determination in mice. The pioneer element CNS3, which acts to potently increase the frequency of T_{reg} cells generated in the thymus and the periphery, binds c-Rel in *in vitro* assays. In contrast, CNS1, which contains a TGF- β -NFAT response element, is superfluous for tT_{reg} cell differentiation, but has a prominent role in iT_{reg} cell generation in gut-associated lymphoid tissues. CNS2, although dispensable for *Foxp3* induction, is required for *Foxp3* expression in the progeny of dividing T_{reg} cells. *Foxp3* binds to CNS2 in a Cbf- β -Runx1 and CpG DNA demethylation-dependent manner, suggesting that *Foxp3* recruitment to this ‘cellular memory module’ facilitates the heritable maintenance of the active state of the *Foxp3* locus and, therefore, T_{reg} lineage stability. Together, our studies demonstrate that the composition, size and maintenance of the T_{reg} cell population are controlled by *Foxp3* CNS elements engaged in response to distinct cell-extrinsic or -intrinsic cues.

To determine *cis*-elements that are potentially involved in the control of T_{reg} cell fate, we first examined permissive (mono-methylated histone H3 at Lys4 (H3K4me1), di-methylated H3K4 (H3K4me2), H3K4me3, H3K36me3, and acetylated H3K9/14 (H3K9/14Ac)) and non-permissive (H3K9me2, H3K9me3 and H3K27me3) modifications of histone H3 bound to three *Foxp3* CNS elements (CNS1–3; Fig. 1a) in CD4⁺CD25⁻*Foxp3*⁻ naive T cells (T_N),

Correspondence and requests for materials should be addressed to A.Y.R. (rudenska@mskcc.org).

[†]Present address: Salk Institute for Biological Studies, La Jolla, California 92037, USA

*These authors contributed equally to this work.

Full Methods and any associated references are available in the online version of the paper at www.nature.com/nature.

Supplementary Information is linked to the online version of the paper at www.nature.com/nature.

Author Contributions Y.Z. and S.J. performed and analysed the experiments, with assistance from A.C. in oligonucleotide pull-down and from X.P.P. in ChIP experiments. K.F. assisted with blastocysts injections. S.J., Y.Z. and A.Y.R. designed experiments and wrote the paper.

Author Information Reprints and permissions information is available at www.nature.com/reprints. The authors declare no competing financial interests.

CD4⁺CD25⁺Foxp3⁺ T_{reg} cells, and B220⁺ B cells isolated from C57BL/6 mice (Fig. 1b–e and data not shown). Chromatin immunoprecipitation (ChIP) showed 5'-end enrichment for H3K4me3 and H3K9/14Ac—chromatin marks characteristic of actively transcribed genes⁵—at the *Foxp3* locus exclusively in T_{reg} cells (Fig. 1b, c). Notably, discrete peaks of H3K4me2 and H3K4me1, but not H3K4me3, were observed at CNS3 in Foxp3⁺ CD4 T cells, but not in B cells (Fig. 1c–e). Furthermore, H3K4me1 was also markedly enriched at CNS3 in CD4⁺CD8⁻Foxp3⁻ and CD4⁺CD8⁺Foxp3⁻ thymocyte subsets serving as thymic T_{reg} precursors (Fig. 1f). These H3K4 features, characteristic of active or poised distal regulatory elements^{6,7}, suggested that CNS3 facilitates Foxp3 induction during thymic and peripheral T_{reg} cell differentiation. Recent studies suggested that synergistic binding of Smad3 and NFAT to CNS1, and binding of both CREB and STAT5 to CNS2, are essential for Foxp3 induction^{8–10}. However, the absence of permissive CNS1- and CNS2-associated chromatin features in T_{reg} precursors indicated that CNS3 probably acts earlier than these two elements during Foxp3 induction.

In silico analysis of CNS3 revealed a motif (AGAAAATCC), resembling the CD28 response element (CD28RE) in the *Il2* locus, known to bind c-Rel homodimers¹¹ (Fig. 1g). Using nuclear extracts of stimulated T_N cells, we demonstrated c-Rel binding to the full-length CNS3 probe, the core CD28RE-like CNS3 element, and the IL2 CD28RE (positive control), but not to a full-length CNS3 probe containing a mutated CD28RE-like sequence (Fig. 1h). Neither p50 (also known as Nfkb1) nor p65 (also known as Rela) bound the core CNS3 CD28RE-like sequence (Fig. 1h and data not shown) suggesting that c-Rel binds to CNS3 as a homodimer. CNS3 did not show enhancer activity in a luciferase reporter assay, in contrast to the stimulation-dependent increase in luciferase activity in the presence of CNS2 and the TGF-β-dependent increase in the presence of CNS1 (Supplementary Fig. 1)^{8,9}. Thus, it is possible that CNS3 binding by c-Rel after its T-cell receptor (TCR)- and CD28-induced activation may facilitate opening of the *Foxp3* locus in a manner similar to its function in the remodelling and activation of the *Il2* locus¹¹.

To determine the *in vivo* function of the three CNS elements, we generated mice containing individual CNS deletions combined with insertion of a green fluorescent protein (GFP) reporter: *Foxp3*^{ΔCNS1-gfp} (CNS1-KO), *Foxp3*^{ΔCNS2-gfp} (CNS2-KO) and *Foxp3*^{ΔCNS3-gfp} (CNS3-KO) (Supplementary Fig. 2). CNS deletions did not cause gross alterations in histone modifications or DNA methylation across the *Foxp3* locus, suggesting that its overall organization was not non-specifically perturbed (Supplementary Figs 3 and 4). Consistent with the hypothesis that CNS3 acts as a pioneer element, we observed a ~5-fold decrease in the frequency of Foxp3⁺ CD4 single-positive (CD4SP) thymocytes with CNS3 deletion, whereas the amount of Foxp3 on a per cell basis was unaffected (Fig. 2a and Supplementary Figs 5 and 6). Marked decreases in CNS3-deficient T_{reg} cells were also observed in female *Foxp3*^{ΔCNS3-gfp/wt} heterozygous mice containing CNS3-deficient and -sufficient Foxp3⁺ cells, whereas control heterozygous *Foxp3*^{gfp/wt} mice expressed each allele at roughly equal frequencies (Supplementary Fig. 7). Notably, numbers of proliferating Ki67⁺Foxp3⁺ thymocytes and peripheral cells were increased in CNS3-KO mice compared to controls (Fig. 2b). Thus, expansion of small numbers of Foxp3⁺ cells is partially compensating a severe impairment in Foxp3 induction in the absence of CNS3. Consistent with this notion, peripheral T_{reg} cell frequencies were only moderately diminished in *Foxp3*^{ΔCNS3-gfp} mice (Fig. 2a and Supplementary Fig. 5). It seems unlikely that this recovery was due to increased generation of iT_{reg} cells because we observed substantial impairment in TGF-β-mediated Foxp3 induction in CNS3-deficient peripheral CD4 T_N cells (Supplementary Fig. 8). Therefore, CNS3 potently increases the probability of *Foxp3* gene expression during thymic and peripheral differentiation of T_{reg} cells.

To evaluate the cell-intrinsic role of c-Rel in the induction of Foxp3 we transferred bone marrow cells from Ly5.2⁺ wild-type, c-Rel-KO, or CNS3-KO mice, mixed at a 1:1 ratio with bone marrow from Ly5.1⁺ wild-type mice, into irradiated *Rag1*^{-/-} recipients. In the resulting chimaeras, c-Rel-deficient thymocytes and peripheral T cells showed severely impaired Foxp3 expression similar to CNS3-KO cells, whereas wild-type precursors generated Foxp3⁺ T_{reg} cells at expected frequencies (Fig. 2c, d and data not shown). These results indicate that c-Rel, activated in response to TCR and CD28 triggering, engages the poised regulatory element CNS3 to facilitate Foxp3 expression and T_{reg} cell differentiation.

Recent studies have suggested that TGF-β may be important for the differentiation of both thymic and peripheral T_{reg} cells^{8,12}. However, we found that *Foxp3*^{ΔCNS1-gfp} mice have no defect in tT_{reg} generation (Fig. 3a). Furthermore, female heterozygous *Foxp3*^{ΔCNS1-gfp/wt} mice contain equal frequencies of CNS1-deficient and -sufficient CD4SP and CD4⁺ CD8⁺ double-positive Foxp3⁺ thymocytes (Supplementary Fig. 9). Thus, CNS1 is dispensable for thymic T_{reg} cell differentiation. However, we observed markedly impaired *in vitro* induction of Foxp3 in CNS1-deficient T_N cells (Fig. 3b). To examine peripheral induction of Foxp3 *in vivo*, we co-transferred CNS1-sufficient and -deficient Ly5.2⁺ CD4 T_N cells with wild-type Ly5.1⁺ T_{reg} cells into T-cell-deficient recipients. CNS1-deficient CD4 T_N cells were defective in their ability to induce Foxp3, that is, generate iT_{reg} cells, most prominently in gut-associated lymphoid tissues (GALT) (Fig. 3c). These observations led us to examine the frequency of Foxp3⁺ T_{reg} in GALT and mesenteric lymph nodes (MLN)—sites of TGF-β-dependent iT_{reg} generation—in unmanipulated *Foxp3*^{ΔCNS1-gfp} mice. Although Foxp3⁺ T_{reg} cell numbers were largely unaffected in the spleen and non-gut draining lymph nodes in *Foxp3*^{ΔCNS1-gfp} mice, we observed a marked decrease in the size of the CNS1-deficient T_{reg} subsets in GALT and MLN compared to littermate controls (Fig. 3d and Supplementary Fig. 10). Furthermore, we failed to observe a characteristic age-dependent increase in the frequency of T_{reg} cells in the absence of CNS1 (Fig. 3d and Supplementary Fig. 10). This defect was due to impaired iT_{reg} generation, because we did not observe any defect in the ability of mature CNS1-KO T_{reg} cells to maintain Foxp3 expression after their transfer into lymphopenic recipients (Supplementary Fig. 11). Together these studies indicate that CNS1 is critical for peripheral induction of Foxp3, occurring primarily in GALT and MLN. The profound defect in iT_{reg} generation in CNS1-KO mice suggests that CNS1 functions solely in the induction of Foxp3 in peripheral CD4 T_N cells in response to TGF-β, probably in cooperation with CNS3.

Despite impaired iT_{reg} cell generation and significantly reduced T_{reg} cell presence in GALT, no significant immune-mediated lesions were observed in the colon, small intestine, or elsewhere in CNS1-KO mice up to 1 year of age (Supplementary Fig. 12). These observations were rather unexpected considering the current view that a block in iT_{reg} differentiation should result in increased inflammation owing to enhanced T_H17 differentiation. However, despite a marked decrease in Foxp3⁺ cells in the MLN of CNS1-deficient mice, the frequencies of T_H17 cells were unaffected, but IL10-producing Foxp3⁻ (Tr1) cell numbers were increased (Supplementary Fig. 13). This observation raises an intriguing possibility that Tr1 and iT_{reg} cells represent alternative fates of T-cell differentiation, and that their immunoregulatory function may be partially redundant in GALT. In agreement with this idea, we found comparable weight loss in CNS1-deficient and -sufficient mice in both acute and chronic models of dextran sulphate sodium (DSS)-induced colitis (Supplementary Fig. 14). Thus, our results indicate different mechanistic requirements for the differentiation of peripheral and thymic T_{reg} cells and their distinct biological functions.

Owing to the non-permissive chromatin configuration at CNS2 in Foxp3⁻ cells and the methylated state of CNS2 CpG motifs in both Foxp3⁻ T cells and in *in vitro* generated Foxp3⁺ iT_{reg} cells¹³, we expected CNS2 to function primarily in 'mature' T_{reg} cells, in which this CpG island is demethylated. Indeed, *Foxp3*^{ΔCNS2-gfp} mice exhibited normal numbers of

Foxp3⁺ thymocytes and Foxp3 expression on a per cell basis (Fig. 4a and Supplementary Fig. 15), and showed unimpeded TGF- β -dependent Foxp3 induction (Supplementary Fig. 16). However, the frequency of Foxp3⁺ T_{reg} cells was significantly decreased among splenocytes of 6-month-old or older (Fig. 4a), but not younger, CNS2-deficient mice (data not shown), suggesting a role for CNS2 in the maintenance of Foxp3 expression in mature T_{reg} cells. To examine this possibility, we co-transferred fluorescence-activated cell sorting (FACS)-purified CNS2-deficient or -sufficient Ly5.2⁺ Foxp3⁺ T_{reg} cells with wild-type Ly5.1⁺ Foxp3⁻ T_N cells into T-cell-deficient recipients. Indeed, CNS2 deficiency markedly impaired maintenance of Foxp3 expression (Fig. 4b and Supplementary Fig. 17). In contrast, CNS1- and CNS3-deficient T_{reg} cells were not compromised in their ability to maintain Foxp3 expression (Supplementary Fig. 11 and data not shown). Furthermore, division of carboxy fluorescein succinimidyl ester (CFSE)-labelled CNS2-deficient T_{reg} cells stimulated with CD3 and CD28 antibodies in the presence of IL2 resulted in a progressive decrease in the frequency of Foxp3⁺ cells and amount of Foxp3 per cell, whereas wild-type T_{reg} cells showed expected increases in both (Fig. 4c). Thus, CNS2 is responsible for heritable Foxp3 expression in dividing mature T_{reg} cells and resembles ‘cellular memory modules’ regulating gene expression during *Drosophila* development¹⁴.

Next, we sought to explore the *trans*-acting factors that may facilitate heritable maintenance of Foxp3 expression after binding to CNS2. CREB and STAT5, previously reported to bind CNS2 (refs 8, 15), were unlikely candidates because retroviral expression of a dominant-negative mutant of CREB in T_{reg} cells did not affect Foxp3 expression, and the STAT5-deficient T_{reg} population isolated from *Foxp3^{Cre}Stat5^{fl/fl}* mice maintained frequencies of Foxp3⁺ cells similar to wild-type controls when transferred into T_{reg}-depleted recipients (data not shown). In contrast, GFP⁺ Foxp3-null T cells (T_{FN}) expressing a *Foxp3* reporter ‘null’ allele (*Foxp3^{gfpko}*), exhibit unstable GFP expression³. To determine whether T_{FN} cells have a similar defect to CNS2-deficient T_{reg} cells in the maintenance of Foxp3 expression we transferred purified GFP⁺ T_{FN} cells, or GFP⁺ T_{reg} cells from *Foxp3^{gfp}* or *Foxp3^{ΔCNS2-gfp}* mice together with Ly5.1⁺ CD4 T cells into T-cell-deficient recipients. A profound decrease in the frequency of GFP⁺ T_{FN} and CNS2-deficient T_{reg} cells in comparison with CNS2-sufficient T_{reg} cells (Supplementary Fig. 18) suggested a potential role for Foxp3 in maintaining its own expression through binding to CNS2. Indeed, Foxp3 from T_{reg} nuclear extracts bound robustly to CNS2 probes (Fig. 4d), and Foxp3 ChIP showed its occupancy of CNS2 in T_{reg} cells (Fig. 4e). Because both demethylation of the CpG island in CNS2 and Foxp3 binding to CNS2 are associated with stable expression of Foxp3, we next explored whether CNS2 demethylation is dependent on Foxp3 binding and vice versa. In GFP⁺ T_{FN} cells lacking Foxp3 protein, and in wild-type T_{reg} cells, CNS2 was similarly demethylated (Fig. 4f), suggesting that CpG demethylation within CNS2 is not dependent on Foxp3. Furthermore, Foxp3 was not bound to CNS2 in purified Foxp3⁺ iT_{reg} cells, whereas Foxp3 binding to a control Foxp3 target gene, *Pde3b*, was readily detectable by ChIP (Fig. 4g). In agreement with previous findings⁹, the CNS2 CpG island remained methylated in iT_{reg} cells (Fig. 4f). Additionally, Foxp3 failed to bind to fully methylated CNS2 probes *in vitro* (Fig. 4h). These results indicate that Foxp3 binding to CNS2 occurs after, and is dependent on, demethylation of CNS2, and suggests that the lack of stable Foxp3 expression in iT_{reg} cells may be attributable to a lack of CNS2 demethylation-dependent Foxp3 autoregulation.

Recent studies showed that Foxp3 protein forms large complexes that include Runx1–Cbf- β ¹⁶. Similar to T_{FN} cells lacking Foxp3 protein and CNS2-deficient T_{reg} cells, Cbf- β -deficient T_{reg} cells progressively lose Foxp3 expression after transfer into lymphopenic mice¹⁷. We found that, as with Foxp3, Runx1–Cbf- β binding to CNS2 (refs 18, 19) was CpG demethylation dependent (Fig. 4h). Fine mapping of the Foxp3–Runx1–Cbf- β complex binding site by Foxp3 ChIP and quantitative PCR (qPCR) using primer sets that tile CNS2 sequence at 200-base-pair (bp) intervals localized the Foxp3-binding peak to a small region containing a conserved

Runx1-binding motif (Fig. 4i and Supplementary Fig. 19). Foxp3 binding to this region was impaired in Cbf- β -deficient T_{reg} cells, suggesting that Foxp3 binds to CNS2 in a Runx1- and Cbf- β -dependent manner (Fig. 4i). In contrast, Foxp3 binding to control target genes (*Nt5e* and *Irf2*) was not affected in the absence of Cbf- β (Fig. 4i). Thus, it seems probable that maintenance of the active state of the *Foxp3* locus in the progeny of dividing T_{reg} cells is dependent on recruitment of Foxp3–Runx1–Cbf- β complexes to CNS2 after demethylation of the CNS2 CpG island. The proposed recruitment of a lineage-determining factor, such as Foxp3, to a cellular memory module element, which becomes accessible only in a fully differentiated state, represents a simple strategy to ensure the stability of cell fate.

Methods Summary

Mice

C57BL/6 (B6) and Ly5.1⁺ B6 congenic mice were purchased from the Jackson Laboratory; *Foxp3^{gfp}* mice have been previously described²⁰. Generation of *Foxp3* CNS1 knockout *Foxp3 Δ CNS1-gfp*, CNS2 knockout *Foxp3 Δ CNS2-gfp*, and CNS3 knockout *Foxp3 Δ CNS3-gfp* mice are described in Methods. Relative to the Foxp3 transcription start site, locations of deleted CNS regions are: CNS1, +2003 to +2707; CNS2, +4262 to +4787; and CNS3, +6909 to +7103. All mice were maintained in the University of Washington SPF animal facility in accordance with institutional regulations.

Cell isolation

CD4⁺CD25⁻ naive T cells, CD4⁺CD25⁺ regulatory T cells and B220⁺ B cells were purified from B6 mouse lymph nodes and spleens using magnetic beads (Miltenyi Biotec). Foxp3–GFP⁺ and Foxp3–GFP⁻ cells were isolated by sorting on a FACS-Aria cell sorter (Becton Dickinson).

Foxp3 induction assay

In vitro Foxp3 induction was performed using FACS-sorted CD4⁺CD62L^{hi} Foxp3–GFP⁻ naive T cells from *Foxp3^{gfp}* or CNS-KO mice co-cultured with irradiated Ly5.1⁺ wild-type T-cell-depleted splenocytes for 3 days in the presence of soluble CD3 antibody (1 μ g ml⁻¹) and TGF- β (2 ngml⁻¹), after which Foxp3 and CD4 expression were assessed by flow cytometry.

In vivo T_{reg} maintenance assay

Five-hundred-thousand FACS-sorted Ly5.1⁻CD4⁺Foxp3–GFP⁺ T_{reg} cells from *Foxp3^{gfp}* or CNS-KO mice were co-injected with 2.5 \times 10⁶ Ly5.1⁺CD4⁺CD62L^{hi}Foxp3–GFP⁻ naive T cells from *Foxp3^{gfp}* into *Rag1^{-/-}* recipient mice. Four weeks after transfer, Ly5.1⁻Foxp3⁺ and Ly5.1⁻Foxp3⁻ cell populations were analysed by flow cytometry.

dsDNA probe pull-down and western blot analysis

Nuclear lysates were prepared from CD4⁺CD25⁺ T_{reg} cells or CD4⁺CD25⁻ T_N cells isolated *ex vivo* or stimulated for 24h with plate-bound CD3 and CD28 antibodies (1 μ g ml⁻¹) in the presence of TGF- β (2 ng ml⁻¹). After pre-clearance using streptavidin-conjugated magnetic beads (Invitrogen), nuclear lysates were incubated with biotinylated dsDNA probes (Supplementary Table 1) followed by incubation with streptavidin-conjugated beads each for 30min at 4°C. After 2–4 washes, the precipitated proteins were subjected to SDS–PAGE and western blot analysis.

Methods

Mice

C57BL/6 and Ly5.1⁺ B6 congenic mice were purchased from the Jackson Laboratory. *Foxp3^{gfp}* mice have been previously described²⁰. All mice were maintained in the University of Washington SPF animal facility in accordance with institutional regulations.

Generation of *Foxp3* CNS knockout mice

All three CNS-targeting constructs were generated on the basis of the previously described *Foxp3^{gfp}* construct¹. For CNS2 and CNS3 constructs, a 8.5-kb SphI fragment of the *Foxp3* gene containing exons 1–7 was obtained from a cosmid containing the complete *Foxp3* genomic sequence. DNA containing enhanced GFP (eGFP) coding sequence was PCR amplified to delete the stop codon and add an NheI site at the 5' end and an AvrII site at 3' end at the same time. The modified eGFP open reading frame (ORF) was subcloned in-frame into the AvrII site in exon1 of the *Foxp3* gene to generate the *Foxp3^{gfp}* construct.

Starting from the *Foxp3^{gfp}* construct, the CNS2-targeting construct was made by insertion of a FRT-PGK-Neo-BGHpA-FRT-LoxP cassette at a ClaI site 5' of CNS2, and a single *loxP* sequence insertion at a NcoI site 3' of CNS2 (Supplementary Fig. 2).

The CNS3-targeting construct was generated by modifying the *Foxp3^{gfp}* construct in two steps. First, a single *loxP* sequence was inserted into the XhoI site upstream of CNS3. Because of the absence of a unique restriction enzyme site, a recombineering technique²¹ was used to insert the FRT-PGK-Neo-BGHpA-FRT-LoxP cassette downstream of CNS3. The principle and protocol of recombineering are described in detail at <http://recombineering.ncicrf.gov/>. Two recombineering arms flanking the insertion point downstream of CNS3 were PCR cloned into a PL451 shuttle vector. A single recombineering step was carried out using standard protocol to insert the FRT-PGK-Neo-BGHpA-FRT-LoxP cassette downstream of CNS3 (Supplementary Fig. 2).

To generate the CNS1 construct, a further 2kb *Foxp3* genomic DNA was inserted upstream of the 8.5-kb SphI fragment. An eGFP cassette was inserted in-frame as described earlier. Three recombineering steps were used to insert *loxP* and the FRT-PGK-Neo-BGHpA-FRT-LoxP cassette flanking CNS1 region. First, a *loxP*-Neo-*loxP* cassette was inserted upstream of CNS1 using a PL452 shuttle vector. Second, the Neo cassette was popped out in a CRE-recombinase-inducible *Escherichia coli* strain, leaving behind a single *loxP* site upstream of CNS1. Third, a FRT-PGK-Neo-BGHpA-FRT-LoxP cassette was inserted downstream of CNS1 using a PL451 shuttle vector.

All CNS-targeting constructs were electroporated into embryonic stem (ES) cell line R1, and selected for G418 and diphtheria-toxin-resistant colonies. Positive ES cell clones were first screened out by PCR, and confirmed by Southern blot. Confirmed positive ES cell clones were injected into B6 blastocysts to generate chimaerical mice, which are then bred with B6 mice for germ-line transmission. CNS-targeted germ-line transmitted mice were bred with FLPeR mouse, which carries FLP recombinase expressed under control of the ROSA26 locus, to delete the Neo cassette and generate CNS-floxed alleles. Finally, CNS-floxed mice were bred with Mox2-Cre mouse, which carries CRE recombinase expressed under control of the *Meox2* (also known as *Mox*) locus, to induce germ-line deletion of CNS regions to generate CNS knockout mice.

Cell isolation

CD4⁺CD25⁻ naive T cells, CD4⁺CD25⁺ T_{reg} cells and B220⁺ B cells were purified from B6 mouse lymph nodes and spleens using MACS isolation kits as per the manufacturer's protocol (Miltenyi Biotec). Peripheral Foxp3-GFP⁺ and Foxp3-GFP⁻ CD4⁺ T cells and Foxp3-GFP⁻ CD4⁺CD8⁻ and Foxp3-GFP⁻ CD4⁺CD8⁺ thymocytes were isolated by sorting on a BD FACS-Aria cell sorter.

In vitro Foxp3 induction and stability assays

In vitro Foxp3 induction assays were performed using FACS-Aria sorted CD4⁺CD62L^{hi} Foxp3-GFP⁻ naive T cells from *Foxp3^{gfp}* or CNS-KO mice. Naive CD4 T cells were co-cultured with irradiated Ly5.1⁺ T-cell-depleted splenocytes for 3 days in the presence of soluble anti-CD3 antibody (1 µg ml⁻¹) and TGF-β (2 ng ml⁻¹), before being stained with anti-CD4 antibody and analysed by flow cytometry. For CFSE-labelled T_{reg} cell stimulation assays, FACS-sorted Foxp3-GFP⁺ T_{reg} cells (>98% purity) were labelled with CFSE (5 µM) in serum-free RPMI for 10 min at 37°C before washing with cold complete RPMI containing 10% FBS. Labelled T_{reg} cells were cultured for 3 days in 96-well plates with plate-coated CD3 and CD28 antibodies (1 µg ml⁻¹) in the presence of recombinant IL2 (500U ml⁻¹). Cells were stained with CD4 and Foxp3 antibodies before flow cytometry analysis.

In vivo T_{reg} maintenance assay

Five-hundred-thousand FACS-Aria sorted Ly5.1⁻CD4⁺ Foxp3-GFP⁺ T_{reg} cells from *Foxp3^{gfp}* or CNS-KO mice were co-injected with 2.5 × 10⁶ Ly5.1⁺CD4⁺CD62L^{hi} Foxp3-GFP⁻ naive T cells from Ly5.1⁺*Foxp^{gfp}* mice into *Rag1^{-/-}* recipient mice. Four weeks after cell transfer, Ly5.1⁻Foxp3⁺ and Ly5.1⁻Foxp3⁻ cell populations in recipient mice were analysed by flow cytometry.

dsDNA probe pull-down and western blot analysis

Ex vivo isolated CD4⁺CD25⁺ T_{reg} cells or CD4⁺CD25⁻ T cells were either unstimulated or stimulated for 24 h with plate-coated anti-CD3 and anti-CD28 antibodies (1 µg ml⁻¹) in the presence of TGF-β (2 ng ml⁻¹). Cells were then lysed and nuclear extracts were made. Extracts were pre-cleared using streptavidin-conjugated magnetic beads (Invitrogen) for 30 min at 4 °C, followed by incubation with biotinylated dsDNA probes (Supplementary Table 1) for 30 min at 4 °C on a rotator. Magnetic streptavidin beads were then added to the extracts and incubated at 4 °C for 30 min. The beads were collected using a magnet and washed two to four times. 2×SDS-loading buffer was added and the extracts were subjected to SDS-PAGE and western blot analysis.

Sequence conservation analysis

Comparisons of mouse *Foxp3* genomic sequences to human, rat and dog were conducted using VISTA algorithm (visualization tool for alignment)²² according to the instruction on the VISTA website (<http://genome.lbl.gov/vista/index.shtml>).

ChIP and CpG dinucleotide methylation analysis

Foxp3 and histone ChIP have been described previously²³. Antibodies specific for different histone modifications were from Upstate Biotechnology (H3K4me3/me2, H3K9/14ac, H3K9me3 and H3K27me3) and Abcam (H3K4me1, H3K36). The relative abundance of regions of interest in precipitated DNA was measured by qPCR using Power SYBR Green PCR master mix (Applied Biosystems). Real-time PCR primer sequences are listed in Supplementary Table 2. CpG dinucleotide methylation analysis was determined by bisulphite treatment of RNase-treated genomic DNA, followed by PCR amplification and

pyrosequencing (Pyro Q-CpG, Qiagen). Pyro Q-CpG was performed by EpigenDX. Sequences analysed were: *Foxp3* promoter, *Foxp3* CNS2, *Foxp3* 3' region, and *Ppp1r3f* promoter.

Isolation of IEL and LPL cells

Isolation of IEL and LPL cells has been described previously²⁴. In brief, intestine was cut longitudinally and then into 2-cm pieces, washed three times with CMF (Ca²⁺- and Mg²⁺-free HBSS containing 1 mM HEPES, 2.5mM NaHCO₃, and 2% FCS, pH7.3). Washed intestinal pieces were stirred at 37 °C for 20 min in CMF containing 10% FCS and 1 mM dithiothreitol (DTT). IELs in supernatant were filtered through a cell strainer and separated by centrifugation on a 44–67% Percoll gradient. To isolate LPLs, the remaining intestinal pieces were washed three times in cold RPMI, and added to 50 ml of RPMI containing 1 mM MgCl₂, 1 mM CaCl₂, 1× HGPG (111.9 mg ml⁻¹ HEPES, 29.2 mg ml⁻¹ L-glutamine, 1,000U ml⁻¹ penicillin, 1 mg ml⁻¹ streptomycin, and 10 mg ml⁻¹ gentamycin), and 150U ml⁻¹ collagenase. Intestinal pieces were stirred at 37 °C for 1h, and released cells were then filtered through a cell strainer. LPLs were then separated by centrifugation on a 44–67% Percoll gradient.

Supplementary Material

Refer to Web version on PubMed Central for supplementary material.

Acknowledgments

We thank T.-T. Chu and L. Karpik for expert technical assistance and mouse colony management, S. Roh for embryonic stem cell culture and screening, J. Rasmussen and A. Kas for bioinformatics support, A. Beg for providing c-Rel knockout mice, P. Treuting for histopathology analysis, J. Gerard for assistance in luciferase reporter assays, and C. Wilson, S. Tarakhovsky and L.-F. Lu for critical comments on the manuscript. This work was supported by grants from the National Institutes of Health (to A.Y.R.). Y.Z. and A.C. were supported by the CRI-Irvington Institute postdoctoral fellowship. S.Z.J. was supported by the CRI pre-doctoral training grant. A.Y.R. is an investigator with the Howard Hughes Medical Institute.

References

1. Sakaguchi S, Yamaguchi T, Nomura T, Ono M. Regulatory T cells and immune tolerance. *Cell* 2008;133:775–787. [PubMed: 18510923]
2. Zheng Y, Rudensky AY. Foxp3 in control of the regulatory T cell lineage. *Nature Immunol* 2007;8:457–462. [PubMed: 17440451]
3. Gavin MA, et al. Foxp3-dependent programme of regulatory T-cell differentiation. *Nature* 2007;445:771–775. [PubMed: 17220874]
4. Williams LM, Rudensky AY. Maintenance of the Foxp3-dependent developmental program in mature regulatory T cells requires continued expression of Foxp3. *Nature Immunol* 2007;8:277–284. [PubMed: 17220892]
5. Ruthenburg AJ, Allis CD, Wysocka J. Methylation of lysine 4 on histone H3: intricacy of writing and reading a single epigenetic mark. *Mol Cell* 2007;25:15–30. [PubMed: 17218268]
6. Birney E, et al. Identification and analysis of functional elements in 1% of the human genome by the ENCODE pilot project. *Nature* 2007;447:799–816. [PubMed: 17571346]
7. Heintzman ND, et al. Distinct and predictive chromatin signatures of transcriptional promoters and enhancers in the human genome. *Nature Genet* 2007;39:311–318. [PubMed: 17277777]
8. Tone Y, et al. Smad3 and NFAT cooperate to induce *Foxp3* expression through its enhancer. *Nature Immunol* 2007;9:194–202. [PubMed: 18157133]
9. Kim HP, Leonard WJ. CREB/ATF-dependent T cell receptor-induce *FoxP3* gene expression: a role for DNA methylation. *J Exp Med* 2007;204:1543–1551. [PubMed: 17591856]
10. Burchill MA, Yang J, Vogtenhuber C, Blazar BR, Farrar MA. IL-2 receptor β -dependent STAT5 activation is required for the development of Foxp3⁺ regulatory T cells. *J Immunol* 2007;178:280–290. [PubMed: 17182565]

11. Rao S, Gerondakis S, Woltring D, Shannon MF. c-Rel is required for chromatin remodeling across the IL-2 gene promoter. *J Immunol* 2003;170:3724–3731. [PubMed: 12646638]
12. Liu Y, et al. A critical function for TGF- β signaling in the development of natural CD4⁺CD25⁺Foxp3⁺ regulatory T cells. *Nature Immunol* 2008;9:632–640. [PubMed: 18438410]
13. Polansky JK, et al. DNA methylation control *Foxp3* gene expression. *Eur J Immunol* 2008;38:1654–1663. [PubMed: 18493985]
14. Murance C, Paro R. A cellular memory module conveys epigenetic inheritance of hedgehog expression during *Drosophila* wing imaginal disc development. *Genes Dev* 2002;16:2672–2683. [PubMed: 12381666]
15. Yao Z, et al. Nonredundant roles for Stat5a/b in directly regulating *Foxp3*. *Blood* 2007;109:4368–4375. [PubMed: 17227828]
16. Ono M, et al. *Foxp3* controls regulatory T-cell function by interacting with AML1/Runx1. *Nature* 2007;446:685–689. [PubMed: 17377532]
17. Rudra D, et al. Runx-CBF β complexes control expression of the transcription factor *Foxp3* in regulatory T cells. *Nature Immunol* 2009;10:1170–1177. [PubMed: 19767756]
18. Kitoh A, et al. Indispensable role of the Runx1-Cbf β transcription complex for *in vivo*-suppressive function of *Foxp3*⁺ regulatory T cells. *Immunity* 2009;31:609–620. [PubMed: 19800266]
19. Bruno L, et al. Runx proteins regulate *Foxp3* expression. *J Exp Med* 2009;206:2329–2337. [PubMed: 19841090]
20. Fontenot JD, et al. Regulatory T cell lineage specification by the forkhead transcription factor *Foxp3*. *Immunity* 2005;22:329–341. [PubMed: 15780990]
21. Lee EC, et al. A highly efficient *Escherichia coli*-based chromosome engineering system adapted for recombinogenic targeting and subcloning of BAC DNA. *Genomics* 2001;73:56–65. [PubMed: 11352566]
22. Dubchak I, Ryaboy DV. VISTA family of computational tools for comparative analysis of DNA sequences and whole genomes. *Methods Mol Biol* 2006;338:69–89. [PubMed: 16888351]
23. Zheng Y, et al. Genome-wide analysis of *Foxp3* target genes in developing and mature regulatory T cells. *Nature* 2007;445:936–940. [PubMed: 17237761]
24. Sather BD, et al. Altering the distribution of *Foxp3*⁺ regulatory T cells results in tissue-specific inflammatory disease. *J Exp Med* 2007;204:1335–1347. [PubMed: 17548521]

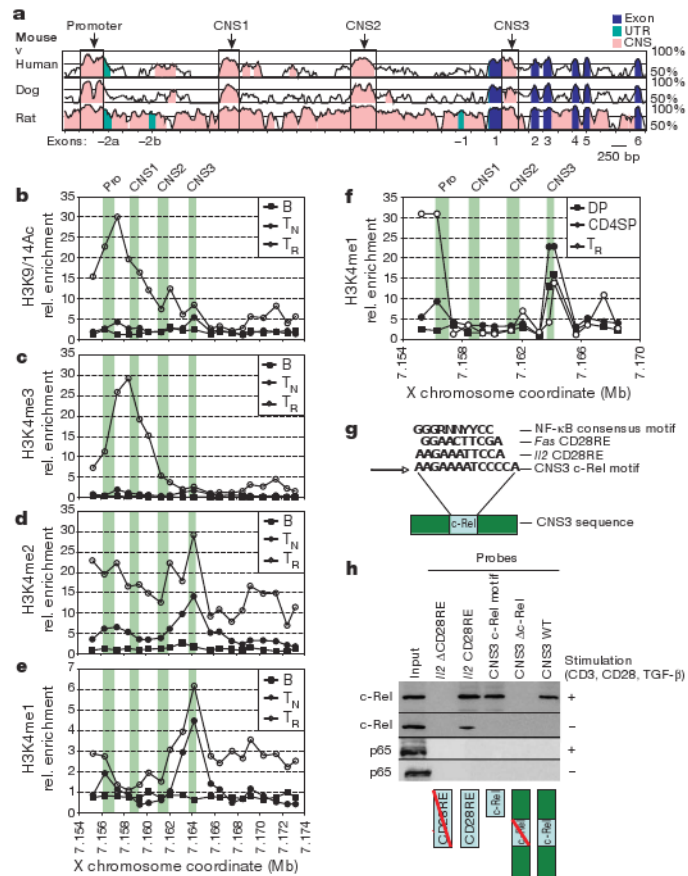


Figure 1. Conserved non-coding sequences and chromatin modifications at the *Foxp3* locus
a, Comparison of mouse *Foxp3* genomic sequence to human, dog and rat. **b-e**, Map of permissive chromatin modifications at the *Foxp3* locus by ChIP-qPCR with primers spaced at ~1-kb intervals for B220⁺ B cells (B), CD4⁺CD25⁻ T_N cells, and CD4⁺CD25⁺ T_{reg} (T_R) cells. Relative (rel.) enrichment data are shown for H3K9/14Ac (**b**), H3K4me3 (**c**), H3K4me2 (**d**) and H3K4me1 (**e**). **f**, H3K4me1 ChIP-qPCR as in **e**, for CD4⁺CD8⁺ (double positive, DP) and CD4⁺CD8⁻ (CD4 single positive, CD4SP) thymocytes, and T_{reg} cells. In **b-f**, green bars denote the promoter (Pro) and CNS1-3. **g**, NF-κB consensus motif in CNS3 (core motif in bold) and homologous CD28RE motifs from *I/2* and *Fas*. N, any base; R, purine; Y, pyrimidine. **h**, Binding of NF-κB family member c-Rel but not p65 to the CD28RE-like element at CNS3. Nuclear lysates from unstimulated or stimulated (1 μg ml⁻¹ CD3 and CD28 antibodies, 2 ng ml⁻¹ TGF-β) T_N cells were incubated with biotinylated double-stranded (ds)DNA probes containing the full-length CNS3 sequence (CNS3 WT), the full-length CNS3 sequence with the mutated core c-Rel motif (CNS3 Δc-Rel), the core CNS3 c-Rel motif, *I/2* CD28RE (positive control), and *I/2* ΔCD28RE (negative control). dsDNA probes and bound protein were precipitated by streptavidin beads and subjected to c-Rel and p65 western blot analysis.

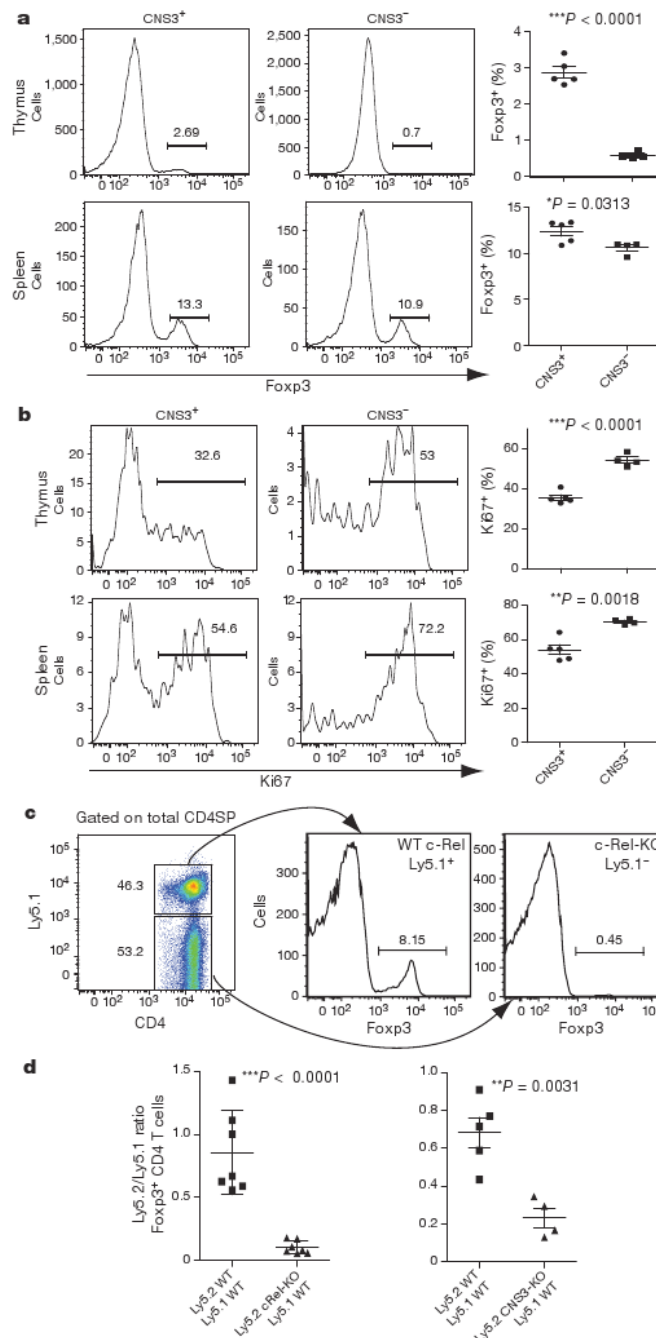


Figure 2. CNS3 controls *de novo* Foxp3 expression

a, Frequency of Foxp3⁺ T_{reg} cells among CD4⁺CD8⁻ cells from thymus and spleen of 2-week-old CNS3-KO mice or littermate controls. **b**, Frequency of Ki67⁺ dividing thymic or splenic Foxp3⁺ T_{reg} cells from same mice as in **a**. **c**, **d**, Analysis of c-Rel-KO (Ly5.2) and wild-type (WT; Ly5.1) mixed bone marrow chimaeras and CNS3-KO (Ly5.2) and wild-type (Ly5.1) mixed bone marrow chimaeras. **c**, Frequency of Foxp3 expressing cells among CD4SP thymocytes of wild-type (Ly5.1⁺) or c-Rel-KO (Ly5.2⁺) origin. **d**, Ratio of Ly5.2⁺ (wild-type and c-Rel-KO, left, or wild-type and CNS3-KO, right) cells to Ly5.1⁺ (wild-type) cells within thymic CD4SP Foxp3⁺ population. Error bars (**a**, **b**, **d**) denote mean \pm s.d.

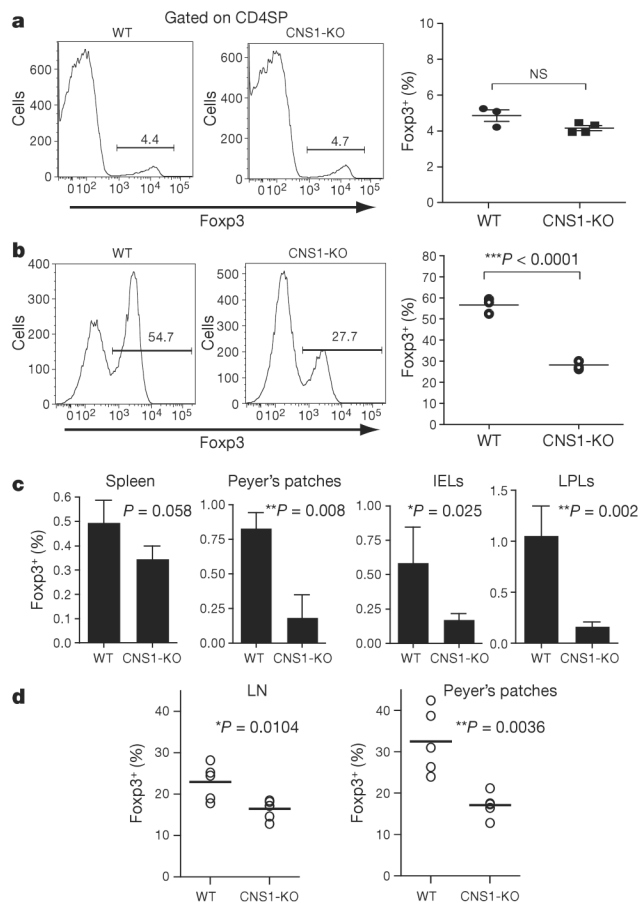


Figure 3. CNS1 controls peripheral, but not thymic, induction of Foxp3 expression

a, Frequency of Foxp3⁺ T_{reg} cells among thymic CD4SP cells in CNS1-KO mice or littermate controls. NS, not significant. **b**, Frequency of Foxp3⁺ iT_{reg} cells generated after stimulation of T_N cells from CNS1-KO or littermate control mice with anti-CD3 (1 μg ml⁻¹), TGF-β (2 ng ml⁻¹) and Ly5.1⁺ irradiated (20 Gy) T-cell-depleted splenocytes for 72h. **c**, Frequency of *in vivo* generated Foxp3⁺ iT_{reg} cells among CD4⁺ cells in spleen, Peyer's patches, intraepithelial lymphocytes (IELs), and lamina propria lymphocytes (LPLs). CNS1-KO or wild-type Ly5.2⁺CD4⁺Foxp3⁻ naive T cells were co-transferred with wild-type Ly5.1⁺Foxp3⁺ T_{reg} cells into T-cell-deficient recipient mice. Ten weeks later, Ly5.2⁺Foxp3⁺ cell populations were analysed by flow cytometry. Error bars denote mean ± s.d. **d**, Frequency of Foxp3⁺ T_{reg} cells among CD4⁺ T cells in peripheral lymph nodes (LN; 'non-mesenteric'), and Peyer's patches of 8–11-month-old CNS1-KO or littermate control mice.

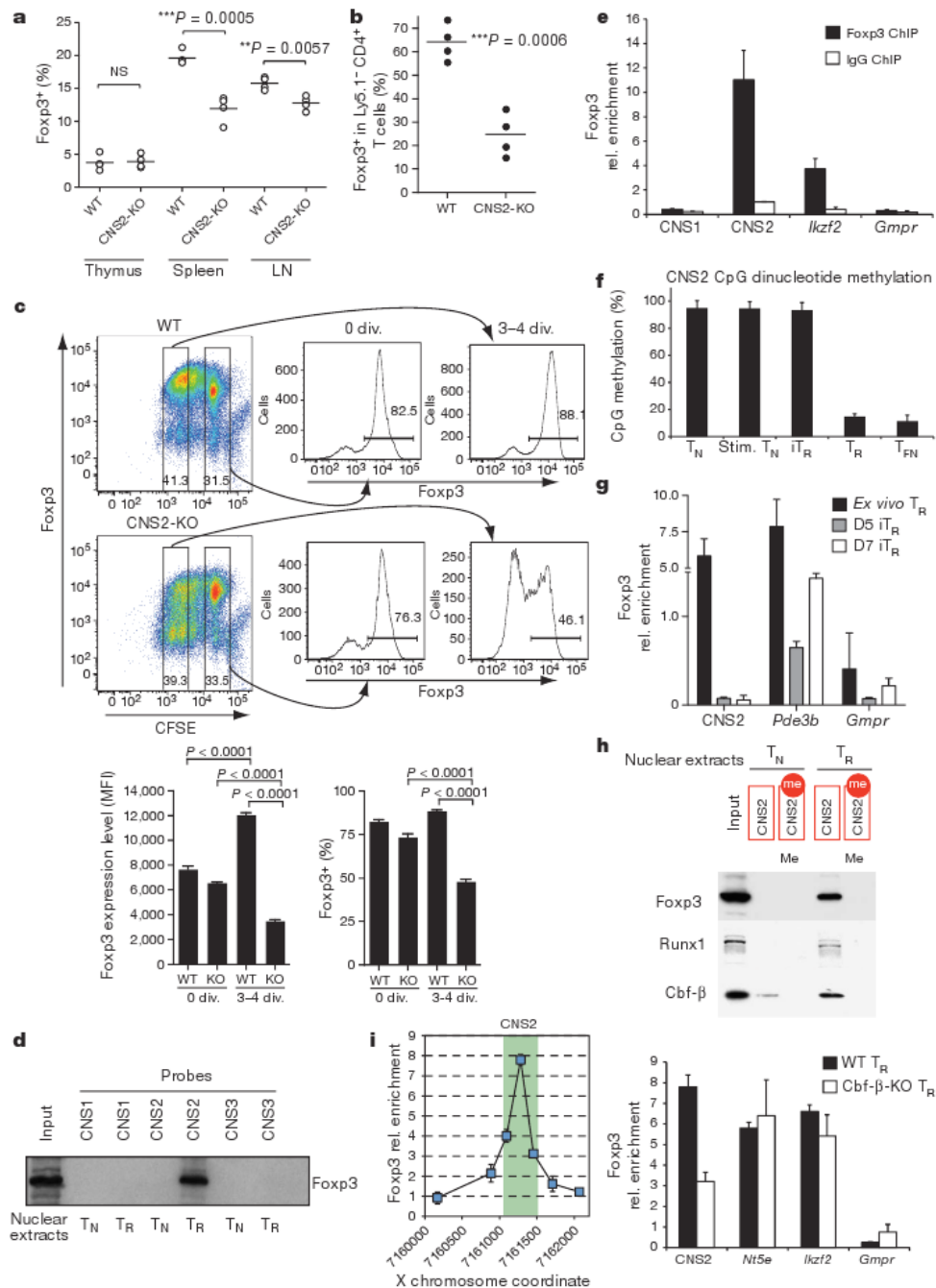


Figure 4. CNS2 controls the heritable maintenance of Foxp3 expression

a, Frequency of Foxp3⁺ T_{reg} cells among CD4SP thymocytes or splenic and lymph node CD4⁺ cells in 6-month-old CNS2-KO mice or littermate controls. **b**, Maintenance of Foxp3 expression in T_{reg} cells from Ly5.2⁺ CNS2-KO or wild-type mice 4 weeks after co-transfer with wild-type Ly5.1⁺CD4⁺Foxp3⁻ cells into T-cell-deficient recipient mice. **c**, Cell division (div.) results in lower Foxp3 expression level and frequency in CNS2-KO T_{reg} cells compared to wild-type T_{reg} cells. CFSE-labelled CNS2-KO or wild-type Foxp3⁺ T_{reg} cells were cultured *in vitro* for 3 days before flow cytometric analysis of Foxp3 expression. MFI, mean fluorescence intensity. **d**, Foxp3 binds to dsDNA probes containing CNS2 sequences. Biotinylated dsDNA probes containing CNS1–3 sequences were incubated with nuclear

extracts from T_N or T_R cells, precipitated with streptavidin beads and subjected to Foxp3 western blot analysis. **e**, Anti-Foxp3 ChIP was performed using wild-type $CD4^+CD25^+$ T_{reg} cells to detect Foxp3 binding to CNS regions *in vivo*. The Foxp3 target gene *Ikzf2* was used as a positive control, *Gmpr* as a non-Foxp3-binding negative control. **f**, Percentages of CpG dinucleotide methylation at CNS2 determined by bisulphite pyrosequencing in T_N cells, T_N cells stimulated for 72 h with anti-CD3 and anti-CD28 antibodies (stim. T_N), purified Foxp3⁺ induced T_{reg} (iT_R, T_N stimulated as above with 2 ng ml⁻¹ TGF-β), $CD4^+CD25^+$ T_{reg} (T_R) cells, and T_{FN} from *Foxp3^{gfpko}* mice. **g**, Foxp3 ChIP at CNS2, the Foxp3 target gene *Pde3b* (positive control), and *Gmpr* (negative control) in *ex vivo* T_{reg} cells and iT_{reg} cells collected on days (D) 5 and 7 of culture with 1 μg ml⁻¹ plate-bound CD3 and CD28 antibodies and 2 ng ml⁻¹ TGF-β. **h**, CpG methylation-sensitive-binding of Foxp3, Runx1 and Cbf-β was determined using methylated and demethylated biotinylated dsDNA CNS2 probes incubated with nuclear extracts from T_N and T_R before streptavidin precipitation and western blot analysis as in **d**. **i**, High-resolution Foxp3 ChIP-qPCR at CNS2 (for primer sequences see Supplementary Table 2) (left) and Foxp3 ChIP in wild-type and Cbf-β-deficient T_{reg} cells from *Cbfb^{fl/fl}Foxp3^{Cre}* mice (right). Green bar denotes the CNS2 region. Foxp3 binding to *Nt5e* and *Ikzf2* served as positive and to *Gmpr* as negative controls. Error bars (**c**, **e-g**, **i**) denote mean ± s.d.